Proceedings of the ASME 2010 29th International Conference on Ocean, Offshore and Arctic Engineering
OMAE 2010
June 6-11, 2010, Shanghai, China

OMAE2010-21071

EVALUATION OF CRITICAL CONDITIONS IN OFFSHORE VESSEL OPERATION BY RESPONSE BASED OPTIMIZATION PROCEDURES

Günther F. Clauss
Ocean Engineering Division
Technical University Berlin
Germany
clauss@naoe.tu-berlin.de

Marco Klein*
Ocean Engineering Division
Technical University Berlin
Germany
klein@naoe.tu-berlin.de

Florian Sprenger
Ocean Engineering Division
Technical University Berlin
Germany
f.sprenger@naoe.tu-berlin.de

Daniel Testa
Ocean Engineering Division
Technical University Berlin
Germany
testa@naoe.tu-berlin.de

ABSTRACT

During the design process of floating structures, different boundary conditions have to be taken into account. Besides the basic determination of the type of vessel, the range of application and the main dimensions at the initial stage, the reliability and the warranty of economical efficiency are an inevitable integral part of the design process. Model tests to evaluate the characteristics and the performance of the floating structure are an important milestone within this process. Therefore it is necessary to determine an adequate test procedure which covers all essential areas of interest. The focus lies on the limiting criteria of the design such as maximum global loads, maximum relative motions between two or more vessels or maximum accelerations, at which the floating structure has to operate or to survive. These criteria are typically combined with a limiting characteristic sea state (H_s, T_p) or a rogue wave. However, the important question remains: What is the worst case scenario for each design parameter - the highest rogue wave or a wave group of certain frequency? And which sea states have to be taken into account for the experimental evaluation of the limiting criteria? As an approach to these challenges, a response based wave generation tool for critical wave sequence detection is introduced. By means of this procedure, model tests can be conducted more efficiently. Besides the theoretical background of the response based wave generation tool, an exemplary practical application for a multi-body system is shown with maximum relative motions as the limiting criterion.

INTRODUCTION

Productivity and survivability are critical parameters for offshore construction design. Modern computer-based analysis technique allow calculation and simulation of these parameters in the design stage, but nevertheless model tests are indispensable for validating the respective approaches. The central problem that has to be solved in the design process of maritime structures is the choice of environmental design conditions to be considered: What are the maximum wave heights? Is the wave of maximum height the worst possible case or are wave groups more dangerous? Of course, this issue cannot be solved globally, i.e. different operating conditions (transit, operation, survival) and characteristics (body motions, local and global loads) will lead

*Address all correspondence to this author.

to individual results. In order to verify the calculated parameters sought, sophisticated model tests are required. Since complex sea states as wave groups have to be generated as exact as possible but with the least amount of time and money, only experienced test facilities are capable of conducting such experimental series.

Linear frequency-domain analysis, i.e. the calculation of RAOs (Response Amplitude Operators), is a basic but fast and elegant approach to investigate the motion characteristics of floating structures prior to model tests [1], which is provided by various numerical tools available. By stochastic analysis procedures, e.g. the annual downtime of offshore production facilities can be calculated on basis of this method. Clauss and Birk [2] proposed a procedure for optimizing buoyancy bodies of floating structures based on linear theory, where the geometry is generated automatically and subsequently analysed linearly and modified to find the minimum of a certain target function (annual downtime). Alford [3] developed an extreme response estimator for the fast evaluation of a new design using an optimization approach to modify the phases of the respective response.

Extreme sea states and their consequences on body motions and loads can be investigated by transferring the linear RAOs into time-domain. Jacobsen and Clauss [4] applied this method to analyse the seakeeping behaviour of multi-body systems. Motions and global loads of a FPSO in extreme sea states were numerically simulated and successfully validated by model tests [5]. Time-domain simulations were used by Clauss et al. [6] to investigate the motion behaviour of a Ro/Ro ferry — especially parametric rolling. It was found that certain wave groups led to a capsize of the vessel.

Besides the analysis of motion behaviour and global loads, the assessment of the maximum number of responses during a structure's lifetime also has to include local loads. Stansberg [7] determined a parameter to assess the risks of slamming at a ship's bow due to waves and wave groups. As already mentioned above, the exact generation and reproduction, respectively, of sea states in a wave tank is an important component of the analysis of floating structures. Fernandes et al. [8] investigated grouping characteristics of waves of the same sea state spectrum and defined the classification into 'Best Sea', 'Mean Sea' and 'Worst Sea'. An experimental optimization procedure for tailor-made wave sequence generation in a wave tank was proposed by Clauss and Schmittner [9], which enables the exact reproduction of wave or wave groups of desired characteristics. Alternatively, the method by Chaplin [10] can be applied to transfer a certain sea state into the wave tank — which was successfully implemented by Schmittner [11] and Schmittner et al. [12] for deterministic wave sequences.

This paper presents a new optimization procedure for the determination of critical situations (i.e. wave sequences) — a response based wave generation tool — combining the advantages of the previously mentioned methods. The response based wave generation tool is exemplarily applied for an innovative offshore LNG — transfer system consisting of a turret moored terminal barge and a shuttle carrier in tandem configuration Fig. (1). This multi-body system is developed within the framework of the joint research project *Maritime Pipe Loading System 20"* (MPLS20) [13], [14]. The limiting parameters are the relative motions of the coupling points of the transfer pipes for LNG on carrier and barge. To ensure a safe unloading process — i. e. avoiding failure of the transfer pipe or even collision — it is indispensable that the maximum tolerable relative motions (relating to the bending capabilities of the pipes) are not exceeded. Therefore a detailed knowledge on the motion characteristics of the carrier and the terminal in tandem configuration is required.

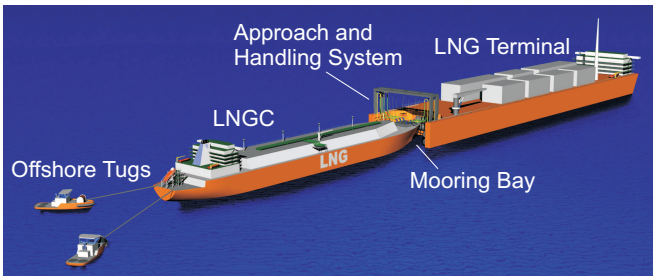

FIGURE 1. TANDEM CONFIGURATION OF THE TURRET MOORED TERMINAL BARGE AND A SHUTTLE CARRIER [13], [14].

THEORETICAL APPROACH

As an idealized case, head waves (β = 180°) are exclusively considered in the following investigations. The focus lies on the transfer configuration with completely filled cargo tanks and the transfer distance of 10 m between terminal stern and carrier bow, which is applied for all investigations. The main dimensions of the terminal and the carrier are shown in Tab. 1.

Both hulls are discretised with a total of 5092 panels for frequency-domain analyses with WAMIT (Wave Analysis at Massachusetts Institute of Technology [15]). WAMIT is widely accepted as a reliable tool for hydrodynamic analyses in offshore technology and proved to be suitable for multi-body problems [4].

At sea states from β = 180°, the motion behaviour of the hydrodynamically coupled bodies is characterized by the RAOs (Response Amplitude Operator) for surge, heave and pitch:

$$H_j(\omega) = \frac{s_{ja}(\omega)}{\zeta_a(\omega)}\, e^{i\,\varepsilon_j(\omega)} \quad \text{with} \quad \begin{array}{ll} j = 1 & \text{for surge} \\ j = 3 & \text{for heave} \\ j = 5 & \text{for pitch,} \end{array} \tag{1}$$

TABLE 1. MAIN DIMENSIONS OF THE LNG CARRIER AND THE TERMINAL

Parameter	Terminal	Carrier
Length over all	360 m (+ 40 m mooring wings)	282 m
Breadth	65 m	42 m
Draught	12 m	12 m
Height	33 m	26 m
Displacement	275087 m^3	103921 m^3

where ω is the angular wave frequency, ζ_a is the wave amplitude, s_{ja} is the amplitude of the respective body motion and ε_j is the corresponding phase angle. The magnitude of this complex number is obtained by $|H_j(\omega)|$.
For the design of the offshore transfer concept, the most critical property is the relative motion between the LNG carrier and the terminal barge in dependency of the environmental conditions. Considering head seas ($\beta = 180°$) exclusively, one point per body is chosen to investigate the relative motion characteristics. First, two new complex RAOs ($H_{x,k}$ and $H_{z,k}$) for each point have to be calculated by the following procedure

$$\begin{bmatrix} H_{x,k}(\omega) \\ 0 \\ H_{z,k}(\omega) \end{bmatrix} = \begin{bmatrix} H_{1,k}(\omega) \\ 0 \\ H_{3,k}(\omega) \end{bmatrix} + \begin{bmatrix} 0 \\ H_{5,k}(\omega) \\ 0 \end{bmatrix} \times \begin{bmatrix} d_{x,k} \\ d_{y,k} \\ d_{z,k} \end{bmatrix} \quad (2)$$

where the original translatory RAOs of each body ($k = 1$ terminal, $k = 2$ carrier) are denoted by $H_{1,k}$ and $H_{3,k}$, the rotatory RAOs by $H_{5,k}$ and the distance between the body fixed coordinate systems and the points of interest by $d_{x,k}$, $d_{y,k}$ and $d_{z,k}$. In order to obtain the relative motions between the two points, the difference of the RAOs for *x*-motions and *z*-motions is calculated

$$H_{l,rel}(\omega) = |H_{l,1}(\omega) - H_{l,2}(\omega)| \text{ with } \begin{matrix} l = 1 \text{ for x direction} \\ l = 2 \text{ for z direction.} \end{matrix} \quad (3)$$

For the subsequent calculations, the connection points of the transfer pipes on the terminal and on the carrier are chosen as illustrated in Fig. 2. Fig. 3 shows the calculated RAO of the relative motion in *z*-direction. On basis of the relative motion RAOs for these points, the operational range of the system — i.e. terminal and carrier in tandem configuration at a distance of 10 m (loading condition) — is determined. The location chosen for this exemplary investigation is Haltenbanken in the Norwegian Sea.

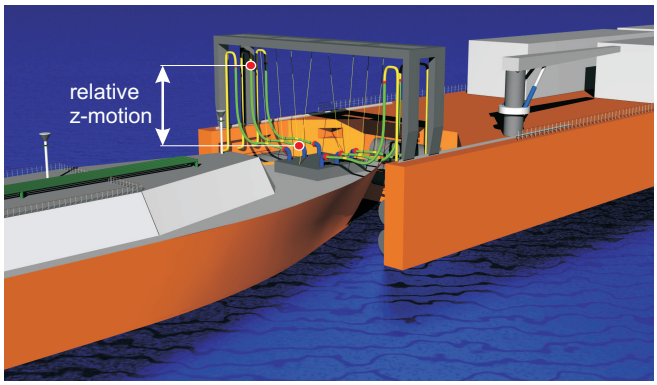

FIGURE 2. ILLUSTRATION OF THE POSITION OF THE CONNECTION POINTS FOR THE LNG TRANSFER PIPE.

At first, a range of JONSWAP spectra with varying zero-upcrossing-periods (0.1 s $\leq T_0 \leq$ 15 s) is multiplied with the squared magnitude of the relative motion RAOs to obtain the response spectra of the relative motions

$$S_{sl,rel}(\omega, T_0) = S(\omega, T_0) \; |H_{l,rel}(\omega)|^2 \quad . \quad (4)$$

Calculating the significant double amplitudes

$$(2s_{l,rel})_s(T_0) = 4 \sqrt{\int_0^\infty S_{sl,rel}(\omega, T_0)\, d\omega} \quad , \quad (5)$$

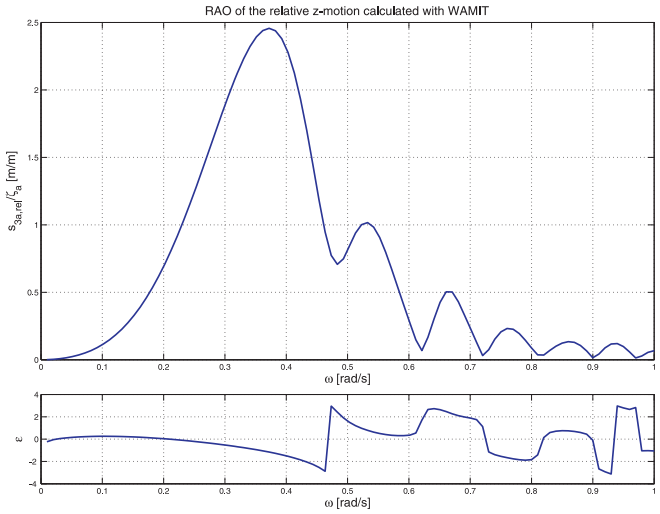

FIGURE 3. MAGNITUDE AND PHASE OF RAO OF RELATIVE Z-MOTIONS OF THE CONNECTION POINTS FOR THE LNG TRANSFER PIPE.

and dividing them by the significant wave height, gives the significant RAOs for the relative motions. For predefined maximum tolerable relative motions (limited by the maximum bending radius of the loading pipe), tolerable significant wave heights are calculated in dependency of the zero-upcrossing-periods

$$(H_{s,tol})_{l,rel}(T_0) = (2s_{l,rel})_{s,tol} \frac{H_s}{(2s_{l,rel})_s(T_0)} \quad , \qquad (6)$$

where the tolerable significant relative motion double amplitudes are given with $(2s_{x,rel})_{s,tol}$ = 2.15 m and $(2s_{z,rel})_{s,tol}$ = 5.38 m — assuming a statistical value of 1.86 for the ratio of tolerable maximum relative motions (horizontal $s_{x,rel} = \pm 2\ m$, vertical $s_{z,rel} = \pm 5\ m$) to tolerable significant relative motions. The data obtained can now be combined with a scatter diagram for the chosen location in order to determine the expected annual downtime. For the following investigations, the vertical relative motions are considered exclusively, resulting in an annual downtime of 1.39 % or 5 days as shown in Fig. 4 where the operational range for the relative z-motion is indicated by the green area. With this data, it is possible to identify critical sea states from a statistical point of view. The next step is to identify the underlying wave sequence which leads to high responses resulting in vertical relative motions which exceed the given limitations. For this purpose the next subsections present three methods for the detection of extreme responses and critical wave sequences including the new approach as follows:

- Random Phase Distribution
- Phase Distribution Optimization
- Response Based Wave Generation Tool

significant wave height Hs [m]	Zero-Upcrossing-Period [s]												Sum
	0-4	4-5	5-6	6-7	7-8	8-9	9-10	10-11	11-12	12-13	13-14	14-15	
11,5-12,0	0	0	0	0	0	0	0	0,006	0	0	0	0	0,006
11,0-11,5	0	0	0	0	0	0	0	0,006	0	0	0	0	0,006
10,5-11,0	0	0	0	0	0	0	0	0,012	0	0	0	0	0,012
10,0-10,5	0	0	0	0	0	0	0	0,006	0	0	0	0	0,006
9,5-10,0	0	0	0	0	0	0	0,012	0,018	0,006	0	0	0	0,036
9,0-9,5	0	0	0	0	0	0	0,06	0,024	0,006	0	0	0	0,090
8,5-9,0	0	0	0	0	0	0	0,078	0,03	0	0	0	0	0,108
8,0-8,5	0	0	0	0	0	0	0,036	0,132	0,018	0	0	0	0,185
7,5-8,0	0	0	0	0	0	0	0,114	0,161	0,03	0	0	0	0,305
7,0-7,5	0	0	0	0	0,018	0,179	0,084	0,006	0	0	0	0	0,287
6,5-7,0	0	0	0	0	0,048	0,365	0,096	0,006	0	0	0	0	0,514
6,0-6,5	0	0	0	0	0,185	0,544	0,042	0,018	0	0	0	0	0,790
5,5-6,0	0	0	0	0	0,7	0,544	0,084	0,006	0	0	0	0	1,334
5,0-5,5	0	0	0	0,042	1,16	0,449	0,102	0	0	0	0	0	1,752
4,5-5,0	0	0	0	0,473	1,531	0,514	0,096	0,006	0	0	0	0	2,620
4,0-4,5	0	0	0,006	1,406	1,621	0,449	0,167	0,012	0	0	0	0	3,661
3,5-4,0	0	0	0,197	2,434	1,573	0,604	0,054	0	0	0	0	0	4,863
3,0-3,5	0	0	1,118	3,074	1,752	0,467	0,096	0	0	0	0	0	6,508
2,5-3,0	0	0,096	3,828	3,84	1,818	0,58	0,09	0,012	0	0	0	0	10,264
2,0-2,5	0	1,854	6,041	4,45	1,693	0,431	0,108	0,018	0	0	0	0	14,594
1,5-2,0	0,496	6,884	6,579	2,991	1,184	0,233	0,042	0	0	0	0	0	18,410
1,0-1,5	4,336	9,57	5,222	2,183	0,419	0,042	0,018	0	0	0	0	0	21,790
0,5-1,0	4,36	4,516	1,962	0,586	0,114	0,018	0	0	0	0	0	0	11,556
0,0-0,5	0,132	0,108	0,054	0,012	0	0	0	0	0	0	0	0	0,305
Sum	9,325	23,028	25,007	21,491	13,817	5,419	1,376	0,478	0,060	0,000	0,000	0,000	100

FIGURE 4. OPERATIONAL RANGE (GREEN) BASED ON MAXIMUM TOLERABLE RELATIVE Z-MOTION FOR THE CONNECTION POINTS OF THE TRANSFER PIPE.

The main assumption of these approaches is that a wave train that creates a large (nonlinear) response in reality is similar to a calculated wave train that creates a large linear response [3, 16]. The first step for all three methods is to select the design sea state. Since this paper focuses on critical wave sequences regarding the maximum relative z-motion of the connection points of the transfer pipe, the limiting operational significant wave height for the MPLS20 system ($H_s = 5.5\ m$) is selected and the respective limiting zero-upcrossing period $T_0 = 9\ s$ is identified from the boundary of the tolerable region in Fig. 4 (yellow rectangle).

Random Phase Distribution

A simple and fast approach to check the maximum occuring relative z-motions of the connection points of the transfer pipe is to calculate the response spectrum $S_{za,rel}(\omega)$ of the relative z-motion for JONSWAP spectra $S(\omega)$ with varying random phases according to Eq.4, and to transfer these spectra into time domain via Inverse Fast Fourier Transformation (IFFT),

$$s_{z,rel}(t) = IFFT(S_{za,rel}(\omega)). \qquad (7)$$

For this purpose a JONSWAP spectrum with $H_s = 5.5\ m$, $T_p = 11.56\ s$ and $\gamma = 3.3$ is chosen, the response in time domain is calculated for 10000 random phase distributions and each response in time domain is analysed regarding the maximum occurring relative z-motion. As a boundary condition the maximum wave height is limited according to $H_{max}/H_s \leq 1.86$ inside the critical wave sequence to be consistent with the previous linear motion analysis. Fig. 5 shows the results of the varying random phase distributions. The top diagram illustrates the maximum relative z-motion per evaluation step. The red dot denotes the maximum relative z-motion ($max(s_{z,rel}(t)) = -5.41\ m$ - cf. bottom diagram) of all evaluation steps. This selected wave scenario is presented in the centre diagram which shows the corresponding surface elevation. The bottom diagram illustrates the associated relative z-motion. The black highlighted sequence and rectangle in the bottom diagram and in particular the wave sequence in the centre diagram display the interval of the surface elevation which is generated and investigated in the seakeeping basin (see Fig. 10 top diagram and Fig. 13). Furthermore this short wave sequence is used as input for the new method, the response based wave generation tool.

Phase Distribution Optimization

So far the worst phase distribution has been determined by random technique. A more straight-forward approach is the optimization of the phase distribution. In this procedure, proposed by

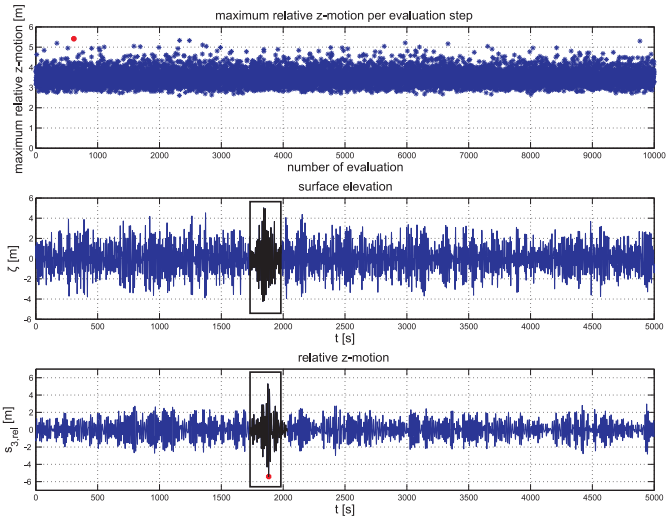

FIGURE 5. RESULTS OF THE VARYING RANDOM PHASE DISTRIBUTION APPROACH.

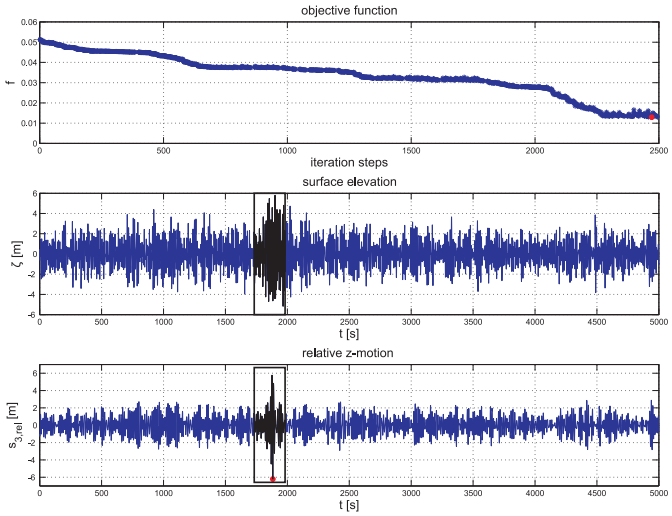

FIGURE 6. RESULTS OF THE PHASE DISTRIBUTION OPTIMIZATION.

Alford [3], a local approach — the Subplex optimization method introduced by Rowan [17] — is used which is a generalization of the Nelder-Mead Simplex method for unconstrained minimization.

The input sea state for the optimization is the sea state obtained in the previous variation of random phase distributions (Fig. 5 - centre diagram). The target parameter of the optimization is the maximization of the motion response between the connection points within a specific time interval (Fig. 5 - black rectangles). The goal of the optimization is to reach an extremely high relative z-motion amplitude. Based on the former result of 5.41 m (see red dots in Fig. 5) this value is set to $s_{max_{z,rel}} = 7\ m$,

$$f = \left(\frac{s_{max_{z,rel}} - max|s_{z,rel}(t)|}{s_{max_{z,rel}}} \right)^2 \tag{8}$$

In addition to the above target parameter, the maximum permissible wave height $H_{max}/H_s \leq 1.86$ within the time interval is defined as inequality constraint, to exclude that the highest responses result from the simplest solution (all component waves are in phase $\rightarrow \zeta_{max} = \sum \zeta_a$).

The optimization procedure starts with the transformation of the sea state in frequency domain via Fast Fourier Transformation (FFT), where the phase angles are modified by the Subplex optimization method. By multiplication with the RAO (Eq. 4) the new response spectra are obtained. Using the Inverse Fourier Transformation to calculate the surface elevation and the respective response in time domain, a zero-upcrossing analysis of the z-motion gives the maximum z-motion value for the calculation of the measure of merit. The optimization process modifies the phase angles until a value of the measure of merit of less than 10^{-6} or 2500 iteration steps are reached.

Fig. 6 shows the results of the optimization procedure. The top diagram shows the measure of merit. It is clearly identifiable that the optimization improves the function f until approximately 2250 iteration steps are reached. Afterwards the optimization fluctuates about the optimum (red dot). For this optimized (worst case) condition the centre diagram shows the wave surface elevation, and the bottom diagram the relative z-motion between the connection points. The maximum relative z-motion at the beginning ($max(s_{z,rel}(t)) = -5.41\ m$) is about $\approx 15\%$ lower than the optimized maximum relative z-motion ($max(s_{z,rel}(t)) = -6.20\ m$). The black highlighted sequence and rectangle in the centre diagram of Fig. 6 displays the interval of the surface elevation which is generated and investigated in the seakeeping basin (see Fig. 10 centre diagram and Fig. 14).

Response Based Wave Generation Tool

The previously presented methods are predestinated for moderate wave heights since nonlinearities of the sea states such as crest-trough asymmetry are not taken into account. The idea of the new optimization concept is based on the previous ones, but the surface elevation is generated automatically using a dedicated nonlinear numerical wave tank to obtain a more realistic surface elevation with respect to the crest-trough asymmetry and wave steepness.

For the simulation of the nonlinear wave propagation a potential theory solver has been developed at Technical University Berlin (WAVETUB) [18, 19]. For the discretization of the fluid domain the Finite Element approach is applied. The two dimensional

nonlinear free surface flow problem is solved in time domain: the fluid is considered inviscid, incompressible, and the flow is irrotational. The atmospheric pressure above the free surface is constant and surface tension is neglected. Hence, the flow field can be described by a velocity potential which satisfies the Laplace equation. At each time step a new boundary-fitted mesh is created and the velocity potential is calculated in the entire fluid domain using the Finite Element method. From this solution the velocities at the free surface are determined by second-order differences. For long term simulations a "numerical beach" is implemented at the end of the wave tank by adding artificial damping terms to the kinematic and dynamic free surface boundary condition in order to suppress reflections. To develop the solution in the time domain the fourth-order Runge-Kutta formula is applied. The procedure is repeated until the desired time step is reached, or the wave train becomes instable due to the occurrence of wave breaking. A complete description of this numerical wave tank is published by Steinhagen [19].

The procedure starts with the surface elevation obtained by the random phase approach as an initial condition. To reduce computational time only a short interval around the maximum response is used - the black highlighted curve in the centre diagram of Fig. 5.

This start-up sequence is transformed backwards to the position of the piston type wave generator by means of linear wave theory. By multiplication with the hydrodynamic transfer function in frequency domain and subsequent Inverse Fast Fourier Transformation a first control signal for the numerical wave tank is obtained. The hydrodynamic transfer function is modelled using the Biesel function [20], relating the wave board stroke to the wave amplitude at the position of the wave maker. The first wave sequence is then calculated in the numerical wave tank and registered at the target position. Fig. 7 shows the results of the first iteration step. The top diagram compares the calculated surface elevation (blue curve) with the initial sea state (red curve). The bottom diagram displays the respective relative z-motion of the connection points of the transfer pipes. Here, the response deviates due to the slightly different surface elevations. Nevertheless, the first control signal and calculated surface elevation is close to the worst case random phase surface elevation and therefore the input for the following optimization.

The wave board stroke (the input of the numerical wave tank) is optimized by the Subplex optimization method [17]. To enable local changes of the wave board stroke, in contrast to the global changes by modifying the phases, the discrete wavelet transformation is introduced into the optimization process. The discrete wavelet transform samples the signal into several decomposition levels and each resulting coefficient describes the wave in a specific time range and frequency bandwidth. Fig. 8 presents the initial control signal of the optimization process and the associated 3-scale discrete wavelet transform. A so-called symlet with 16 coefficients, as introduced by [21], is selected as wavelet. The third decomposition level of the wavelet transform is composed of the approximation coefficients c3 and the detail coefficients d1, d2 and d3 from the previous decomposition levels. Due to the use of the wavelet transform the number of free variables can be significantly reduced if only approximation and detailed coefficients of the third decomposition level c3 and d3 are modified. These coefficients contain most of the wave energy, i.e. they feature the greatest magnitude.

The maximization of the relative z-motion response between the connection points within the simulated time interval is the target parameter and the goal of the optimization is to reach a maximum relative z-motion amplitude (see Eq. 8), which is left $s_{max_{z,rel}} = 7\ m$ since the phase distribution optimization approach does not reach this target value but equals $max(s_{z,rel}(t)) = -6.20\ m$ instead.

In addition to the above target parameter, the inequality constraints

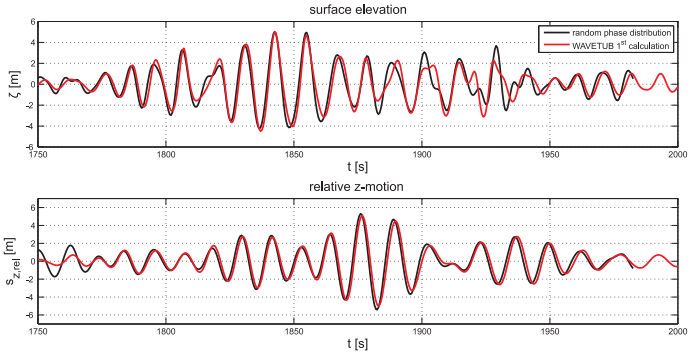

FIGURE 7. COMPARISON OF THE FIRST NUMERICAL CALCULATION WITH WAVETUB (RED CURVE) AND THE RANDOM PHASE DISTRIBUTION APPROACH (BLACK CURVE) OPTIMUM. THE TOP DIAGRAM SHOWS THE SURFACE ELEVATION AND THE BOTTOM DIAGRAM THE ASSOCIATED VERTICAL RELATIVE Z-MOTION.

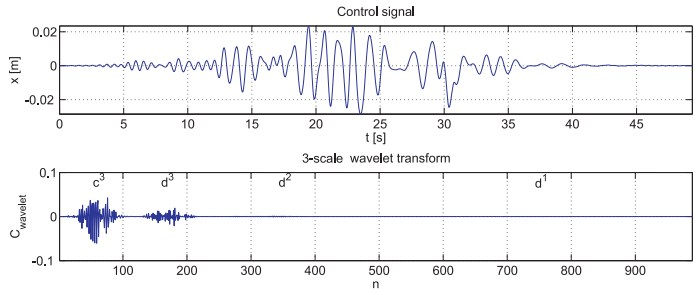

FIGURE 8. CONTROL SIGNAL FOR THE NUMERICAL WAVE BOARD (TOP) AND THE ASSOCIATED 3-SCALE WAVELET TRANSFORM (BOTTOM).

- $H_{max}/H_s \leq 1.86$
- maximum wave board velocity
- maximum wave board acceleration
- termination condition due to instabilities of the numerical calculation (wave breaking)

have to be defined, to ensure a smooth optimization run. Firstly, the wave board stroke is modified at each iteration step, then the numerical calculation is carried out and the registered surface elevation is transformed in the frequency domain and multiplied with the relative z-motion RAO to obtain the relative z-motion. Afterwards the measure of merit (f) is calculated and evaluated by the Subplex algorithm, the wave board stroke is modified, and the next iteration step starts until a value of the measure of merit of less than 10^{-6} or 2500 iteration steps are reached.
Fig. 9 shows the results of the new optimization approach. The top diagram displays the measure of merit. Surprisingly, the objective function decreases very fast and reaches the threshold of $f = 7.5 \cdot 10^{-}7$ after only approximately 350 iteration steps, which is equivalent to a maximum vertical relative motion of $s_{max_{z,rel}} = +7\ m$. This result indicates that the maximum relative motion with the given boundary conditions is greater than $s_{max_{z,rel}} = +7\ m$, so that further investigations with greater target values are necessary. Note that the free areas inside the diagram are associated with inequality constraints ($f = 9$). The centre diagram shows the optimized surface elevation and the bottom diagram the associated relative z-motion. The difference between the maximum relative z-motion of the random phase optimization ($max(s_{z,rel}(t)) = -5.41\ m$) and the optimized maximum relative z-motion ($max(s_{z,rel}(t)) = +7\ m$) is $\approx 27\%$. Thereby the optimization process modifies the surface elevation in such a manner that the maximum relative z-motion changes its algebraic sign regarding the results of the random phase distribution and phase distribution optimization. If in the worst case the carrier bow is in the highest position and the terminal stern in the lowest, the algebraic sign is negative.

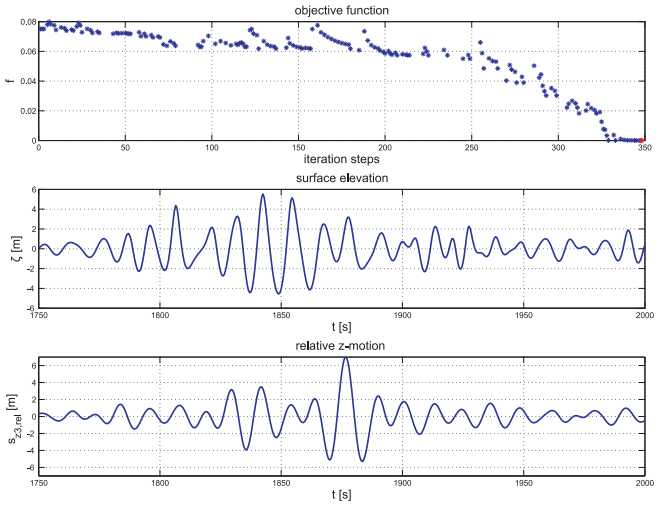

FIGURE 9. RESULTS OF THE RESPONSE BASED WAVE GENERATION TOOL.

EXPERIMENTAL PROGRAM AND RESULTS

The model tests are conducted in the seakeeping basin of the Ocean Engineering Division of Technical University Berlin at a model scale of 1:100. The basin is 110 m long, with a measuring range of 90 m. The width is 8 m and the water depth is 1 m. On the one side an electrically driven piston type wave generator is installed. The wave generator is fully computer controlled and a software is implemented which enables the generation of regular waves, transient wave packages, deterministic irregular sea states with defined characteristics as well as tailored critical wave sequences.

Wave Generation

For the reproduction of a specific wave sequence in the seakeeping basin different approaches have been developed. Depending on the focus of the reproduction, i.e. on the grade of accuracy for the reproduction of a single wave or wave group, either an experimental optimization procedure [9, 16], which enables the exact reproduction of desired characteristics, or a phase-amplitude iteration procedure [11, 12] for fast generation with sufficient accuracy can be applied. In our case the focus lies on a fast reproduction of the wave groups to accelerate the model test procedure, hence the phase-amplitude iteration procedure is applied.
At first, the scaled calculated wave sequence is transformed back to the position of the piston type wave generator by means of linear wave theory. By multiplication with the electrical and hydrodynamic transfer function in frequency domain and subsequent inverse Fourier transformation a first control signal for the wave generator is obtained. The wave sequence is then generated in a physical wave tank and recorded at the target position. Since nonlinear effects like wave-wave interaction and wave breaking may occur during the experiment the measured wave train differs from the target parameters. To improve the accuracy of the reproduced wave sequence at the target location, i.e. to fit the wave train to the target parameters, the control signal is iteratively improved by the phase-amplitude iteration procedure [11, 12].
Fig. 10 compares the calculated surface elevations (black lines) with the measured surface elevations (red lines) in the seakeeping basin. The top diagram shows the result for the random phase distribution approach, the centre diagram the result for the phase distribution optimization and the bottom diagram for the response based wave generation tool. The green ellipse in Fig. 10 denotes the target wave sequence which should be reproduced accurately. The global agreement of the calculated and

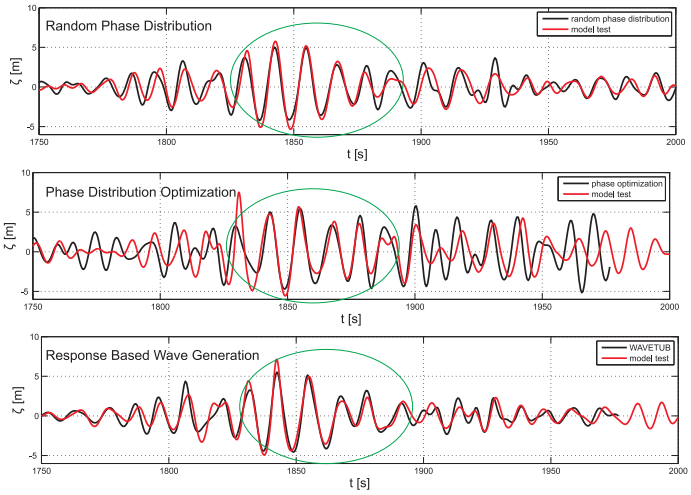

FIGURE 10. COMPARISON OF THE CALCULATED AND MEASURED SURFACE ELEVATIONS OF THE THREE DIFFERENT APPROACHES. THE TOP DIAGRAM FOR THE RANDOM PHASE DISTRIBUTION APPROACH, THE CENTRE DIAGRAM FOR THE PHASE DISTRIBUTION OPTIMIZATION AND THE BOTTOM DIAGRAM FOR THE RESPONSE BASED WAVE GENERATION TOOL.

generated wave sequences is best for the response based wave generation tool (bottom diagram) followed by the random phase distribution (top diagram).

Test Setup

For experimental investigations, a glass-fibre reinforced plastic (GRP) model of the LNG carrier and the terminal barge are built at a scale of 1:100 (see Fig. 11). The carrier model is soft-moored and both vessels are equipped with four wireless, individually pulsed infrared sensors each. The body motions in six degrees of freedom are precisely tracked by five cameras mounted on a carriage above the basin with a tracking range of 8 $\times$ 10 m. Water depth is 1 m, the distance between the two vessels is 0.1 m.

Model Test Results

The results of the three different approaches are validated with model test results. Thereby the tandem configuration of the LNG transfer is investigated by applying the transient wave package technique to validate the calculated relative z-motion RAO and in the sea states generated in the previous section.
Fig. 12 compares the calculated relative z-motion RAO (blue curve) with the relative z-motion RAO measured during the model tests (red curve). The overall agreement is satisfactory, in particular for the phases. The amplitudes of the measured relative z-motion RAO are consistently higher, which can be attributed

FIGURE 11. PICTURE OF THE MODEL TEST SETUP.

to the fact that the influence of the soft mooring arrangement on the restoring behaviour is not taken into account in the numerical simulation. In general, a slight deviation of calculated and measured RAOs, or nonlinear effects have no influence on the optimization process since a maximum value is sought. In our case, the measured relative z-motion is slightly higher than values calculated by the different numerical approaches.
Fig. 13 presents the experimental results for the random phase distribution approach, Fig. 14 for the phase distribution optimization and Fig. 15 for the response based wave generation tool. All

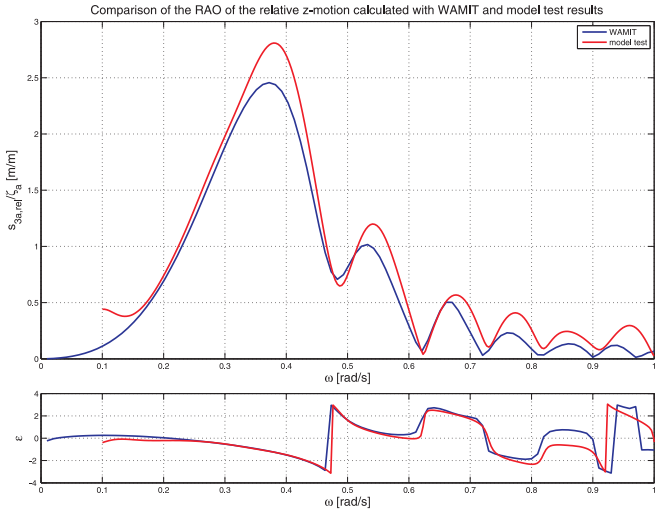

FIGURE 12. COMPARISON OF THE CALCULATED RELATIVE Z-MOTION RAO (BLUE LINE) AND THE RELATIVE Z-MOTION RAO MEASURED DURING THE MODEL TESTS (RED LINE).

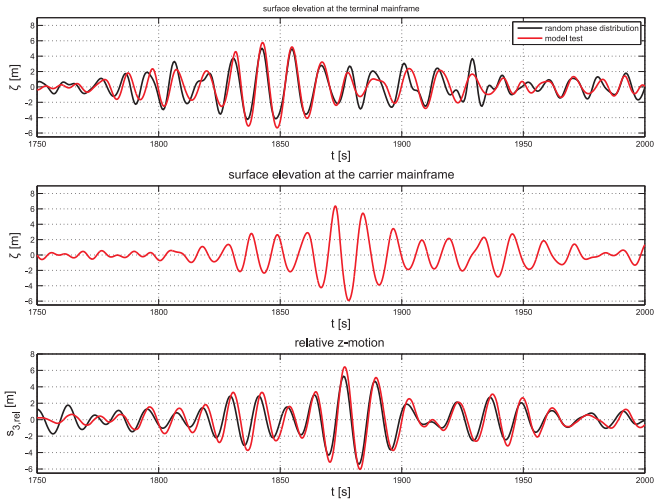

FIGURE 13. COMPARISON OF THE MEASURED AND CALCULATED RESULTS FOR THE RANDOM PHASE DISTRIBUTION APPROACH.

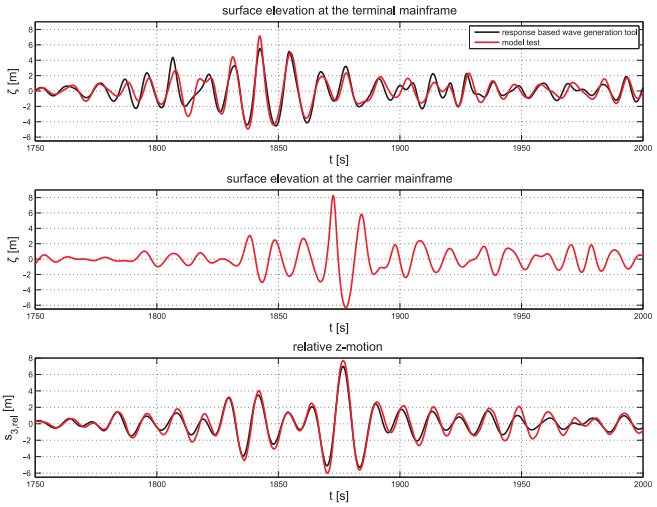

FIGURE 15. COMPARISON OF THE MEASURED AND CALCULATED RESULTS FOR THE NEW RESPONSE BASED WAVE GENERATION TOOL.

three figures are arranged as follows: the top diagram shows the surface elevation at the mainframe of the terminal which is the target location for the calculation and reproduction, the centre diagram shows the surface elevation at the mainframe of the carrier and the bottom diagram shows the relative z-motion of the coupling point of the transfer pipes. The red curves denote the measurement and the black curves the calculated results.

For all three test runs the overall agreement between the calculated and measured relative z-motions is good, but (as already discussed above) the measured magnitudes of the motions are slightly higher than the calculated values. The detected maximum relative z-motion of the three approaches are confirmed by the model tests. Fig. 16 compares the absolute magnitudes of the calculated and measured response for the three approaches. The trend between the different approaches is verified, i.e. for the calculated as well as the measured response, the largest magnitude appears for the new optimization approach.

Having discussed the measurement results, now the mechanisms leading to these large responses are investigated. The centre diagrams of Figs. 13 - 15 show the measured surface elevation at the mainframe of the carrier. Here the input parameters of the approaches must be recalled, where one important boundary condition is that the maximum wave height must not exceed a ratio of $H_{max}/H_S = 1.86$. This maximum wave height limit is defined for the target location of the relative z-motion RAO which is the mainframe of the terminal. So the defined statistical values are satisfied for one location of the two vessels in tandem configuration. However, approx. 335 m behind this location a

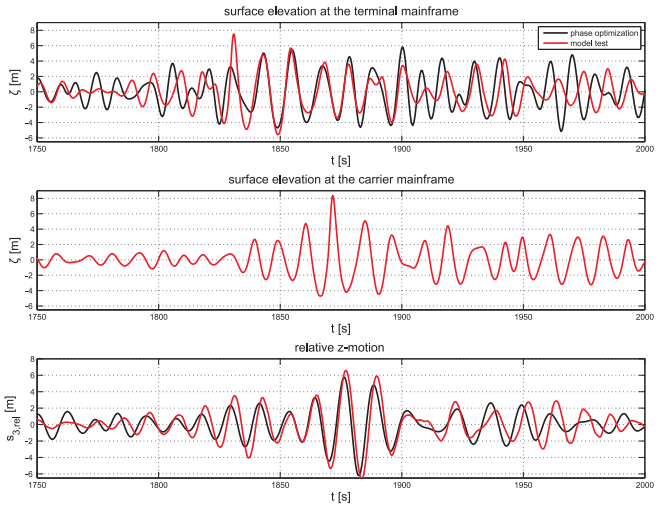

FIGURE 14. COMPARISON OF THE MEASURED AND CALCULATED RESULTS FOR THE PHASE DISTRIBUTION OPTIMIZATION.

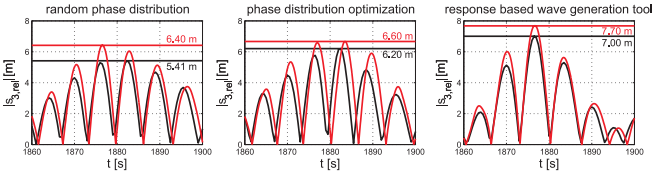

FIGURE 16. COMPARISON OF THE MEASURED AND CALCULATED ABSOLUTE MAGNITUDE FOR THE THREE APPROACHES.

high single wave exceeding $H_{max}/H_s = 1.86$ is developing in the course of the wave propagation. The measured wave height of the detected single wave at the mainframe of the carrier is simultaneously increasing for the three different approaches, i.e. from the random phase approach to the response based model test tool results where the highest wave appears. For the given sea state ($H_s = 5.5\ m$, $T_0 = 9\ s$), the following mechanism can be identified: At the terminal mainframe, a group of high waves close to the wave height limitation and approx. $\omega = 0.57\ rad/s$ is generated. After propagating 335 m, a single high wave exceeding $H_{max}/H_s = 1.86$ evolves at the carrier mainframe with $\omega = 0.57\ rad/s$, which is related to the secondary peak in the vertical relative motion RAO in Fig. 12. This peak is caused by intersection of the single body pitch RAOs for carrier and terminal and lies within a region of significant wave energy for the selected sea state — in contrast to the primary peak at $\omega = 0.37\ rad/s$.

The functional principle of the new response based wave generation tool is introduced and verified with a chosen example of practical relevance, i. e. vertical relative motions between a LNG terminal and a shuttle carrier at loading condition (distance 10 m, wave incident angle $\beta = 180^\circ$). Other incident angles, e. g. $\beta = 150^\circ$ would result in different RAO characteristics with multiple values due to increasing influence of roll motions and hence different wave trains that would lead to high responses. The new tool is also capable to handle multiple target values, e.g. $H_{max}/H_s = 1.86$ at the terminal and the carrier mainframe or different types of target values as wave period or asymmetries (wave steepness) limitations.

CONCLUSIONS

This paper presents a new optimization approach for the identification and evaluation of critical situations prior to model tests. In general, arbitrary RAOs (absolute motion, relative motion, forces and moments, accelerations etc.) can be investigated by this method.

Exemplarily, a multibody system consisting of a LNG carrier and a terminal barge in tandem configuration (transfer distance 10 m, full scale) is analysed. For the investigation of critical situations the relative z-motion of the connection points of the LNG transfer pipe is chosen.

On the one hand, the new approach is compared to a classical design evaluation tool, using random phase distributions. On the other hand, a phase optimization procedure is applied for a straightforward identification of the worst case scenario with regard to a selected sea state. The comparison of the three different procedures shows that the proposed new optimization approach identifies the worst case scenario with regard to the relative z-motion of the connection point of the transfer pipe.

Compared to the model test results, the phase-iteration scheme gives an efficient wave reproduction with sufficient accuracy. In general, it is demonstrated that the trend between the different approaches, regarding the maximum calculated vertical relative motion is verified by the model tests. Furthermore, the good agreement between the model test results and the calculations reveals that the assumption that a wave train creating a large (nonlinear) response in reality is similar to a calculated wave train that creates a large linear response is adequate.

Both optimization approaches are appropriate alternatives to seek critical wave sequences straightforward. Regarding the computational time, the phase distribution optimization is superior to the response based wave generation tool since the calculation with the potential solver WAVETUB is more time consuming (approx. 3 days for 1500 iteration steps on a state-of-the-art PC). Therefore, the phase distribution optimization is more suitable for fast optimization and evaluation of different target parameters with regard to critical wave sequences. But the implementation of WAVETUB has a lot of advantages:

- Realistic, nonlinear surface elevation (crest/trough asymmetry and wave steepness) and propagation
- Exact modelling of the wave tank and wave board → transfer of the numerical wave board motion to the seakeeping basin
- Optimized WAVETUB output can be used directly as input for subsequent CFD calculations [22]

The next steps in the development of the response based wave generation tool is the direct implementation of the numerical wave board motion in experimental analysis which would further improve the test preparation since the iterative wave sequence calibration then becomes dispensable. Furthermore the capability of this tool will be tested with different floating structures and optimization targets.

ACKNOWLEDGMENT

The response based wave generation tool is developed as a contribution to the project EXTREME SEAS, which is founded by the European Commission, under the Grant agreement no. 234175. We highly acknowledge the support of this research project and want to thank our project partners Det Norske Veritas AS, Instituto Superior Técnico, Germanischer Lloyd AG, Meteorological Institute, Universita di Torino, Institute of Applied Physics, Canal de Experiencias Hidrodinamicas de El Pardo, Meyer Werft, Estaleiros Navais Viana de Castelo and University Duisburg-Essen.

The authors also wish to express their gratitude to the German Federal Ministry of Economics and Technology (BMWi) and Project Management Jülich (PTJ) for funding the joint research project '*MPLS20 — Maritime Pipe Loading System 20*"' (FKZ 03SX240D), in particular to Dipl.-Ing. Barbara Grothkopp and Dipl.-Betriebswirtin Cornelia Bude for their excellent support. Furthermore, we want to thank the MPLS20 consortium ('*IMPaC Engineering*','*Brugg Pipe Systems*' and '*Nexans*').

REFERENCES

[1] Clauss, G., Lehmann, E., and Östergaard, C., 1992. *Offshore Structures*, Vol. 1: Conceptual Design and Hydrodynamics. Springer Verlag London.

[2] Clauss, G., and Birk, L., 1996. "Hydrodynamic shape optimization of large offshore structures". *Applied Ocean Research, 18(4)*, August, pp. 157–171.

[3] Alford, L. K., 2008. "Estimating extreme responses using a non-uniform phase distribution". PhD thesis, The University of Michigan.

[4] Jacobsen, K., and Clauss, G. F., 2006. "Time-Domain Simulations of Multi-Body Systems in Deterministic Wave Trains". In OMAE 2006 - 25th International Conference on Offshore Mechanics and Arctic Engineering. OMAE2006-92348.

[5] Clauss, G. F., Schmittner, C. E., Hennig, J., Guedes Soares, C., Fonseca, N., and Pascoal, R., 2004. "Bending Moments of an FPSO in Rogue Waves". In OMAE 2004 - 23rd International Conference on Offshore Mechanics and Arctic Engineering. OMAE2004-51504.

[6] Clauss, G., Hennig, J., and Cramer, H., 2002. "Evaluation of Capsizing Risk by Deterministic Analysis of Extreme Roll Motions". In ITTC 2002 - 23rd International Towing Tank Conference.

[7] Stansberg, C. T., 2008. "A Wave Impact Parameter". In OMAE 2008 - 27th International Conference on Offshore Mechanics and Arctic Engineering. OMAE2008-57801.

[8] Fernandes, A. C., Hennig, J., Maia, M. D., Cozijn, H., and Sales, J. S., 2008. "Worst sea-best sea wave group spectra from random sea states". In OMAE 2008 - 27th International Conference on Offshore Mechanics and Arctic Engineering. OMAE2008-57821.

[9] Clauss, G. F., and Schmittner, C. E., 2005. "Experimental Optimization of Extreme Wave Sequences for the Determinsitic Analysis of Wave/Structure Interaction". In OMAE 2005 - 24th International Conference on Offshore Mechanics and Arctic Engineering. OMAE2005-67049.

[10] Chaplin, J. R., 1996. "On Frequency-Focusing Unidirectional Waves". *International Journal of Offshore and Polar Engineering, 6(2)*, pp. 131–137.

[11] Schmittner, C. E., 2005. "Rogue Wave Impact on Marine Structures". *Dissertation*, Technische Universität Berlin (D 83).

[12] Schmittner, C., Kosleck, S., and Hennig, J., 2009. "A Phase-Amplitude Iteration Scheme for the Optimization of Deterministic Wave Sequences". In OMAE 2009 - 28th International Conference on Ocean, Offshore and Arctic Engineering. OMAE2009-80131.

[13] Clauss, G., Sprenger, F., Testa, D., Hoog, S., and Huhn, R., 2009. "Motion Behaviour of a New Offshore LNG Transfer System at Harsh Operational Conditions". In OMAE 2009 - 28th Conference on Ocean, Offshore and Arctic Engineering.

[14] Hoog, S., Koch, H., Huhn, R., Frohne, C., Homann, J., Clauss, G., Sprenger, F., and Testa, D., 2009. "LNG Transfer in Harsh Environments — Introduction of a New Concept". In Offshore Technology Conference. OTC 19866.

[15] DEPARTMENT OF OCEAN ENGINEERING, MIT, WAMIT, 1994. *WAMIT Version 5.1 – A Radiation-Diffraction Panel Program For Wave-Body Interactions*. Userguide.

[16] Clauss, G. F., 2008. "The Taming of the Shrew: Tailoring Freak Wave Sequences for Seakeeping Tests". In Journal of Ship Research, Vol. 52, Nr. 3, pp. 194–226.

[17] Rowan, T., 1990. "Functional stability analysis of numerical algorithms". PhD thesis, University of Texas at Austin.

[18] Clauss, G. F., and Steinhagen, U., 1999. "Numerical simulation of nonlinear transient waves and its validation by laboratory data". In Proceedings of 9^{th} International Offshore and Polar Engineering Conference (ISOPE), Vol. III, pp. 368–375.

[19] Steinhagen, U., 2001. "Synthesizing Nonlinear Transient Gravity Waves in Random Seas". *Dissertation*, Technische Universität Berlin (D 83).

[20] Biésel, F., and Suquet, F., 1951. "Les apparails générateurs de houle en laboratoire". *La Houille Blanche*(2), Mars-Avril, pp. 147–165.

[21] Daubechies, I., 1988. "Orthonormal bases of compactly supported wavelets". *Communications on Pure and Applied Mathematics*, 41, pp. 909–996.

[22] Clauss, G. F., Schmittner, C. E., and Stück, R., 2005. "Numerical Wave Tank – Simulation of Extreme Waves for the Investigation of Structural Responses". In OMAE 2005 - 24th International Conference on Offshore Mechanics and Arctic Engineering. OMAE2005-67048.